



Oxygen isotopes in tree rings show good coherence between species and sites in Bolivia



Jessica C.A. Baker^{a,*}, Sarah F.P. Hunt^a, Santiago J. Clerici^a, Robert J. Newton^b, Simon H. Bottrell^b, Melanie J. Leng^c, Timothy H.E. Heaton^c, Gerhard Helle^d, Jaime Argollo^e, Manuel Gloor^a, Roel J.W. Brien^a

^a Department of Ecology and Global Change, School of Geography, University of Leeds, Leeds LS2 9JT, UK

^b School of Earth and Environment, University of Leeds, Leeds LS2 9JT, UK

^c NERC Isotope Geosciences Facilities, British Geological Survey, Keyworth, Nottingham NG12 5GG, UK

^d GFZ – German Research Centre for Geosciences, Section 5.2 Climate Dynamics and Landscape Evolution, Telegrafenberg, 14473 Potsdam, Germany

^e Laboratorio de Dendrocronología e Historia Ambiental, Instituto de Investigaciones Geológicas y del Medio Ambiente, Universidad Mayor de San Andrés, Campus Universitario, calle 27 s/n, Cotacota La Paz, Bolivia

ARTICLE INFO

Article history:

Received 22 May 2015

Received in revised form 11 September 2015

Accepted 15 September 2015

Available online 18 September 2015

Keywords:

Tree rings
Oxygen isotopes
Cross-dating
Tropical forest
Bolivia

ABSTRACT

A tree ring oxygen isotope ($\delta^{18}\text{O}_{\text{TR}}$) chronology developed from one species (*Cedrela odorata*) growing in a single site has been shown to be a sensitive proxy for rainfall over the Amazon Basin, thus allowing reconstructions of precipitation in a region where meteorological records are short and scarce. Although these results suggest that there should be large-scale (>100 km) spatial coherence of $\delta^{18}\text{O}_{\text{TR}}$ records in the Amazon, this has not been tested. Furthermore, it is of interest to investigate whether other, possibly longer-lived, species similarly record interannual variation of Amazon precipitation, and can be used to develop climate sensitive isotope chronologies. In this study, we measured $\delta^{18}\text{O}$ in tree rings from seven lowland and one highland tree species from Bolivia. We found that cross-dating with $\delta^{18}\text{O}_{\text{TR}}$ gave more accurate tree ring dates than using ring width. Our “isotope cross-dating approach” is confirmed with radiocarbon “bomb-peak” dates, and has the potential to greatly facilitate development of $\delta^{18}\text{O}_{\text{TR}}$ records in the tropics, identify dating errors, and check annual ring formation in tropical trees. Six of the seven lowland species correlated significantly with *C. odorata*, showing that variation in $\delta^{18}\text{O}_{\text{TR}}$ has a coherent imprint across very different species, most likely arising from a dominant influence of source water $\delta^{18}\text{O}$ on $\delta^{18}\text{O}_{\text{TR}}$. In addition we show that $\delta^{18}\text{O}_{\text{TR}}$ series cohere over large distances, within and between species. Comparison of two *C. odorata* $\delta^{18}\text{O}_{\text{TR}}$ chronologies from sites several hundreds of kilometres apart showed a very strong correlation ($r = 0.80$, $p < 0.001$, 1901–2001), and a significant (but weaker) relationship was found between lowland *C. odorata* trees and a *Polylepis tarapacana* tree growing in the distant Altiplano ($r = 0.39$, $p < 0.01$, 1931–2001). This large-scale coherence of $\delta^{18}\text{O}_{\text{TR}}$ records is probably triggered by a strong spatial coherence in precipitation $\delta^{18}\text{O}$ due to large-scale controls. These results highlight the strength of $\delta^{18}\text{O}_{\text{TR}}$ as a precipitation proxy, and open the way for temporal and spatial expansion of precipitation reconstructions in South America.

© 2015 The Authors. Published by Elsevier B.V. This is an open access article under the CC BY license (<http://creativecommons.org/licenses/by/4.0/>).

1. Introduction

Palaeo proxies allow reconstruction of past climates beyond the limit of instrumental records, and thus help the interpretation of recent and on-going climatic changes. Tree rings have the potential to be particularly useful climate archives: They are widely distributed and often allow reconstructions at annual resolution or higher (Briffa, 1999). In

the tropics, however, it has long been assumed that trees do not form visible growth rings (e.g. Whitmore, 1998). Nonetheless, studies in recent decades show that in fact many tropical tree species do form annual rings, in response to seasonal variation in rainfall (Worbes, 1999), or an annual flood-pulse (Schöngart et al., 2002). Indeed, annual ring formation has been observed and verified in 67 tree species from tropical lowland rainforest alone (Zuidema et al., 2012). Despite these advances, useful tree ring based climate reconstructions are notably scarce from the tropics (see the International Tree-Ring Data Bank; Grissino-Mayer and Fritts, 1997), an important region in terms of global climate. This is due in part to the difficulty of developing climate sensitive proxies from tropical tree species; ring-width patterns often match poorly between trees, making cross-dating a challenge (Groenendijk et al., 2014; Stahle, 1999) and growth responses to interannual climate

* Corresponding author.

E-mail addresses: gyjcab@leeds.ac.uk (J.C.A. Baker), s.f.p.hunt@leeds.ac.uk (S.F.P. Hunt), s.j.clerici@leeds.ac.uk (S.J. Clerici), r.j.newton@leeds.ac.uk (R.J. Newton), s.bottrell@leeds.ac.uk (S.H. Bottrell), mjl@nigl.nerc.ac.uk (M.J. Leng), theh@nigl.nerc.ac.uk (T.H.E. Heaton), ghelle@gfz-potsdam.de (G. Helle), jaimo_argollo@yahoo.es (J. Argollo), egloor@leeds.ac.uk (M. Gloor), r.brien@leeds.ac.uk (R.J.W. Brien).

variation are often relatively weak (e.g. Brienen and Zuidema, 2005; Scholten et al., 2013; van der Sleen et al., 2015; Worbes, 1999) due to generally favourable growth conditions, especially in warm and humid climates. Alternative methods are therefore required in the tropics to extract useful climate information from tree rings.

One promising approach is to use the oxygen isotope composition of tree rings ($\delta^{18}\text{O}_{\text{TR}}$) to reconstruct past precipitation. Unlike variation in ring-width, $\delta^{18}\text{O}_{\text{TR}}$ in several tropical sites have been shown to be highly sensitive to variations in rainfall amount, at local and regional scales (e.g. Anchukaitis and Evans, 2010; Brienen et al., 2012; 2013; Scholten et al., 2013; Xu et al., 2011). In a particularly successful study, a $\delta^{18}\text{O}_{\text{TR}}$ chronology constructed from eight *Cedrela odorata* trees from a single site in northern Bolivia showed a clear signal of precipitation integrated over the whole Amazon Basin, demonstrated by a close correlation between Amazon River discharge at Obidos, Brazil and the $\delta^{18}\text{O}_{\text{TR}}$ record ($r = 0.58$; Brienen et al., 2012). This correlation suggests that *C. odorata* is an excellent recorder of the isotopic composition of precipitation ($\delta^{18}\text{O}_{\text{P}}$), which in turn is a good proxy for basin-wide precipitation. *Cedrela odorata* is a shallow-rooted species (Cintron, 1990), only using water from the top soil (Schwendenmann et al., 2014). Thus the water taken up by the tree (source water) predominantly comes from recent precipitation, and this is probably the reason it so accurately records year-to-year variation in $\delta^{18}\text{O}_{\text{P}}$ (Brienen et al., 2012). $\delta^{18}\text{O}_{\text{P}}$ is itself influenced by several factors which affect the rate of rainfall and return of isotopes to the atmosphere, including the continental effect, altitude effect, amount effect and recycling of water by vegetation (see Dansgaard, 1964; Risi et al., 2008; Rozanski et al., 1993; Salati et al., 1979). In the lowland forest of northern Bolivia, the location of the trees used in this study, cumulative rainfall of heavy isotopes during transport of water vapour across the continent from the Atlantic seems to be the dominant control of variation in $\delta^{18}\text{O}_{\text{P}}$ (i.e. the continental effect; Brienen et al., 2012; Pierrehumbert, 1999; Salati et al., 1979; Sturm et al., 2007). Equilibrium fractionation during condensation in rainclouds results in preferential removal of heavy isotopes during rain events (Dansgaard, 1964) and leads effectively to a Rayleigh distillation process, such that precipitation downwind becomes more and more isotopically depleted. If *C. odorata* indeed records such large-scale effects, one would expect trees from sites several hundreds of kilometres apart to show the same interannual variation in $\delta^{18}\text{O}_{\text{TR}}$. Such coincidence of isotopic variation would not only be helpful in tree ring dating and construction of tree ring chronologies, but would also confirm the case for large-scale effects controlling $\delta^{18}\text{O}_{\text{P}}$ in the Amazon Basin.

Apart from *C. odorata*, the potential for the development of isotope chronologies has thus far been tested for very few tree species in tropical South America (see Ballantyne et al., 2011). Using additional, possibly longer-lived tree species allows for an increase in the spatial and temporal coverage of precipitation reconstructions in South America and beyond. However, it is currently not known to what degree other tree species (with similar and different rooting behaviours) show the same $\delta^{18}\text{O}_{\text{TR}}$ signals because other factors influence $\delta^{18}\text{O}_{\text{TR}}$ besides source water isotopic composition ($\delta^{18}\text{O}_{\text{S}}$). Several of these factors are conceptualized in the mechanistic model presented by Roden et al. (2000) which, as a background, we briefly summarize here.

Starting at the roots, water uptake from the soil is a non-fractionating process, so water reaching the leaves has a very similar isotopic composition to soil water (Ehleringer and Dawson, 1992). In the leaf, water is isotopically enriched relative to the source water. There are two components to this process: Enrichment of heavy water at the site of evaporation in the leaf (due to preferential transpiration of isotopically light water) and back diffusion of some of this heavy water to the rest of the leaf (Barbour et al., 2004; Roden et al., 2000). This second component, the back diffusion of heavy water from the evaporative site, affects the isotope ratio of bulk leaf water ($\delta^{18}\text{O}_{\text{L}}$) and consequently the isotopic signal of cellulose precursors which form throughout the leaf (Sternberg, 2009). The magnitude of back diffusion

of heavy water is primarily determined by the rate of transpiration: Under high (low) transpiration rates, advection of unenriched water from the vein is higher (lower), reducing (increasing) back diffusion, and thus causing $\delta^{18}\text{O}_{\text{L}}$ to be more similar to (more enriched than) $\delta^{18}\text{O}_{\text{S}}$ (Song et al., 2013). The ratio of advective to diffusive transport is known as the Péclet number (Farquhar and Lloyd, 1993) and this has an important moderating influence on $\delta^{18}\text{O}_{\text{L}}$ (and thus the $\delta^{18}\text{O}$ of fixed sugars).

In a final step, the $\delta^{18}\text{O}$ signal of sugars produced in the leaf further changes before conversion to cellulose. Sugars formed in the leaf are transported to the stem where some of the oxygen atoms may exchange with stem water oxygen during cellulose synthesis, determining the final isotope signature (Hill et al., 1995). This exchange is important, as it acts to partially “uncouple” $\delta^{18}\text{O}_{\text{TR}}$ from leaf physiology (Offermann et al., 2011), and reinforces the signal of the source water. Experimental evidence shows that the degree of exchange is positively related to the turnover time of non-structural carbohydrates (Song et al., 2014b), thus leading to differences between species in the degree to which $\delta^{18}\text{O}_{\text{TR}}$ represents $\delta^{18}\text{O}_{\text{S}}$ (Song et al., 2014a).

Several studies have examined how interannual $\delta^{18}\text{O}_{\text{TR}}$ records vary between different temperate tree species, and within and between sites (Li et al., 2015; Marshall and Monserud, 2006; Reynolds-Henne et al., 2009; Saurer et al., 2008; Singer et al., 2013). Coherence in $\delta^{18}\text{O}$ records between species varies considerably. Saurer et al. (2008) analysed six tree species in Switzerland and found a weak common interspecies signal in $\delta^{18}\text{O}_{\text{TR}}$ (mean inter-series correlation = 0.23), with the strongest relationship between spruce and beech ($r = 0.68$). The authors attribute these correlations to temperature influencing $\delta^{18}\text{O}_{\text{S}}$ and an influence of precipitation through its effect on local humidity. Li et al. (2015) found a strong relationship between pine and oak $\delta^{18}\text{O}_{\text{TR}}$ records in Japan ($r = 0.67$), driven by summer precipitation amount controlling $\delta^{18}\text{O}_{\text{S}}$. In other temperate studies trends in $\delta^{18}\text{O}_{\text{TR}}$ differed strongly between species (Marshall and Monserud, 2006; Reynolds-Henne et al., 2009; Singer et al., 2013). These inter-species differences were variously attributed to species-specific partitioning of source water within the soil profile (Marshall and Monserud, 2006; Saurer et al., 2008; Singer et al., 2013), differences in plant physiology (Reynolds-Henne et al., 2009; Saurer et al., 2008), and differences in phenology (Saurer et al., 2008), although isolating the drivers of inter-specific differences in $\delta^{18}\text{O}_{\text{TR}}$ can be a challenge.

This paper focuses on tropical South America and aims: i) to determine whether or not an established Bolivian $\delta^{18}\text{O}_{\text{TR}}$ chronology can be used as a reference curve to verify dating of new isotope records, ii) to assess how well $\delta^{18}\text{O}_{\text{TR}}$ signals correspond between species, and iii) to investigate coherence of $\delta^{18}\text{O}_{\text{TR}}$ signals between distant sites. For this purpose we analyse multi-decadal $\delta^{18}\text{O}_{\text{TR}}$ records for eight tropical tree species from three lowland moist forest sites and one site in the Bolivian Altiplano. Among these are five light-demanding tree species, two shade-tolerant tree species and one high altitude shrub. To address the first question, isotope series that were dated by ring counting were compared with a well-replicated and verified $\delta^{18}\text{O}_{\text{TR}}$ record from Brienen et al. (2012). Dating of re-aligned series was verified using radiocarbon “bomb-peak” dating (Worbes and Junk, 1989). The $\delta^{18}\text{O}_{\text{TR}}$ record for each lowland species was then compared with the geographically closest *C. odorata* chronology to assess interspecies signal correlations. Finally, to assess spatial coherence of $\delta^{18}\text{O}_{\text{TR}}$ signals, *C. odorata* records from lowland sites >300 km apart were first compared with each other, and then with a *Polylepis tarapacana* series from the Altiplano (>1000 km distant).

2. Material and methods

2.1. Study species

We selected eight tropical tree species that form clear and annual rings (Argollo et al., 2004; Brienen and Zuidema, 2005): Seven are

Bolivian lowland rainforest tree species (*C. odorata*, *Tachigali vasquezii*, *Amburana cearensis*, *Peltogyne heterophylla*, *Bertholletia excelsa*, *Cedrelinga catenaeformis* and *Couratari macrosperma*), while one species (*P. tarapacana*) only grows at high altitudes in the Bolivian Altiplano. Hereafter species will be referred to by their generic names only. Ring anatomy for the lowland species (except for *Couratari*) is described in [Brienen and Zuidema \(2005\)](#), and for *Polylepis* in [Argollo et al. \(2004\)](#). Relevant ecological characteristics are described below, and summarized in [Table 1](#).

The lowland species vary in their growth rates and regeneration requirements. *Cedrela*, *Tachigali* and *Cedrelinga* reach the highest diameter growth rates, while *Amburana*, *Peltogyne* and *Bertholletia* show slower diameter growth rates ([Table 1](#)). All of the lowland species, except for *Peltogyne* and *Couratari*, seem to require gaps at some stage during their regeneration, and are classified as light-demanding ([Brienen and Zuidema, 2006](#)). *Peltogyne* is the most shade-tolerant species with the densest wood. Leaf phenology differs between species, from obligate deciduous leaf habit in *Cedrela* and *Amburana*, which lose their leaves for several months, to evergreen or brevi-deciduous in other species. *Cedrela* prefers well-drained soils, has a superficial root system ([Cintron, 1990](#)), and predominantly uses water from the top 30 cm of the soil profile ([Schwendenmann et al., 2014](#)). *Amburana* is often found on deep, well-drained or otherwise calcareous soils ([Leite, 2005](#)) and *Bertholletia* also seems to favour well-drained sites. For the other species, we have very little information on soil preferences or rooting depth. Species also vary in their adult stature – *Bertholletia* and *Cedrelinga* are the tallest species, reaching over 2 m in diameter and heights of up to 50 m (classified as “emergents”), while the other lowland species are canopy trees, growing to maximum heights of 25–35 m.

The only species in this study from the Altiplano, *Polylepis* has the highest altitudinal range of any tree in the world, growing between 3900 and 5200 m elevation ([Solíz et al., 2009](#)). These trees grow slowly due to the cold and dry climate, and can live for over 700 years ([Solíz et al., 2009](#)). Precipitation is the main growth-limiting factor in these dry highlands ([Morales et al., 2004](#)), making *Polylepis* particularly useful for climate reconstructions ([Morales et al., 2004](#); [Solíz et al., 2009](#)). Trees at these altitudes remain small (rarely exceeding 7 m in height; [Domic and Capriles, 2009](#)), and radial growth patterns are often highly eccentric.

2.2. Regional setting

Tree ring samples for this study come from lowland rainforest sites in northern Bolivia, except for the *Polylepis* sample which originated from the Bolivian Altiplano, close to the Sajama volcano at an altitude of 4400–4500 m ([Fig. 1](#); 18°06'S, 68°53'W; [Solíz et al., 2009](#)). The *Amburana* sample is from the private property Purisima, in Pando

(11°24'S, 68°43'W; 170 m.a.s.l.), while the *Tachigali*, *Peltogyne*, *Bertholletia* and *Cedrelinga* samples were obtained from logging concession areas approximately 40 km to the east of the town Riberalta (10°55'S, 65°40'W; 160 m.a.s.l.). These two sites are described by [Brienen and Zuidema \(2005\)](#). The *Couratari* and *Cedrela* samples are from a third lowland site, Selva Negra (10°5'S, 66°18'W; 160 m.a.s.l.), 90 km north of Riberalta and approximately 325 km northeast of the Purisima site. All of the lowland sites have a similar climatology, with total annual precipitation between 1675 and 1850 mm (Cobija and Riberalta station data, GHCN-Monthly version 2, [Peterson and Vose, 1997](#), accessed from Climate Explorer (<http://climexp.knmi.nl>)), and a distinct dry period during the austral winter (June–August) with less than 100 mm of rain per month.

For *Amburana*, *Tachigali*, *Peltogyne*, *Bertholletia* and *Cedrelinga* stem discs were collected between October 2002 and September 2003 from trees that had been felled, or that had died of natural causes (see [Brienen and Zuidema, 2005](#) for sampling protocols). Discs of *Couratari* and *Cedrela* were collected in 2011 from trees felled for timber. The *Polylepis* disc was collected in 2003. Between 5 and 31 discs were collected per species. Sampling height varied between 0.5–2.0 m above the ground, and discs ranged from 30 to 200 cm in diameter.

2.3. Oxygen isotope analysis

Stem discs were collected and polished with sandpaper up to grit 600 using a mechanical sander. Rings were then marked and cross-dated (see [Section 2.4](#) for full description). Old trees with good internal cross-dating were selected for isotope analysis. For *Cedrela* we selected nine trees, while for the other species only one tree was selected. While we acknowledge that a single individual is not sufficient to develop a climate sensitive chronology, this approach is well suited to explore coherence in $\delta^{18}\text{O}_{\text{TR}}$ between different species and a well-developed chronology. Using one tree per species allowed us to maximize the number of species included in this study (see also [Ballantyne et al., 2011](#); [Saurer et al., 2008](#)). Each ring was individually cut up using a scalpel, sampling equally from the entire width of the ring to ensure even representation of the whole growing season. In some instances where rings were very narrow it was not possible to isolate sufficient wood for analysis, and the final isotope series therefore show some missing data-points. We extracted α -cellulose from the wood following the batch method of [Wieloch et al. \(2011\)](#). Cellulose was homogenized using a mixer mill (Retsch MM 301) and then freeze-dried. Samples were then weighed into silver capsules for isotope analysis.

Oxygen isotope data presented here were measured at three different labs: The British Geological Survey's Stable Isotope Facility (part of the NERC Isotope Geosciences Facilities) (NIGF; Keyworth, Nottingham, UK); the School of Earth and Environment (SEE) at the University of

Table 1
Growth strategy, leaf-fall behaviour, adult stature, maximum observed age, maximum growth rate, rooting depth and habitat of the eight study species. Maximum diameter growth rate is the mean of the five highest annual growth rates observed in different trees.

| Species name | Family | Growth strategy | Leaf-fall behaviour | Adult stature | Max. observed age (years) | Max. growth rate (cm year ⁻¹) | Rooting depth | Habitat |
|---------------------------------|---------------|---------------------|---------------------|-----------------|---------------------------|-------------------------------------------|---------------|-----------------------------------|
| <i>Cedrela odorata</i> | Meliaceae | Light-demanding | Obligate deciduous | Canopy | 308 ^a | 3.2 ^a | Shallow | Evergreen – seasonally dry forest |
| <i>Amburana cearensis</i> | Leguminosae | Light-demanding | Obligate deciduous | Canopy | 243 ^a | 1.8 ^a | ? | Evergreen – seasonally dry forest |
| <i>Peltogyne heterophylla</i> | Leguminosae | Shade-tolerant | Brevi-deciduous | Canopy | 254 ^a | 1.8 ^a | ? | Tropical lowland moist forest |
| <i>Tachigali vasquezii</i> | Leguminosae | Light-demanding | Brevi-deciduous | Canopy | 35 ^a | 4.8 ^a | ? | Tropical lowland moist forest |
| <i>Couratari macrosperma</i> | Lecythidaceae | Shade-tolerant | ? | Canopy-emergent | ? | ? | ? | Tropical lowland moist forest |
| <i>Cedrelinga catenaeformis</i> | Leguminosae | Light-demanding | Brevi-deciduous | Emergent | 123 ^a | 3.7 ^a | ? | Tropical lowland moist forest |
| <i>Bertholletia excelsa</i> | Lecythidaceae | Light-demanding | Obligate deciduous | Emergent | 427 ^a | 1.9 ^a | ? | Tropical lowland moist forest |
| <i>Polylepis tarapacana</i> | Rosaceae | High altitude shrub | Evergreen | ? | 705 ^b | ? | ? | Cold, high altitude desert |

^a [Brienen and Zuidema \(2005\)](#).

^b [Solíz et al. \(2009\)](#).



Fig. 1. Map showing the locations of sample sites in this study (circles) and the location of the *Polylepis* chronology from Ballantyne et al. (2011; triangle). The species sampled at each site are as follows: *Cedrela* and *Couratari* from Selva Negra, *Amburana* from Purisima, *Tachigali*, *Peltogyne*, *Bertholletia* and *Cedrelinga* from Riberalta and *Polylepis* from Sajama. The Amazon Basin catchment area is shaded in pale green. Lowland sites are shown in black and Altiplano sites are shown in red. (For interpretation of the references to color in this figure legend, the reader is referred to the online version of this chapter.)

Leeds, UK; and the German Research Centre for Geosciences (GFZ; Potsdam, Germany). Analysis of the *Cedrela* samples was performed at NIGF utilizing a Thermo Finnigan (Bremen, Germany) TC/EA linked to a Delta + XL isotope ratio mass spectrometer (IRMS) at 1400 °C. $^{18}\text{O}/^{16}\text{O}$ ratios were converted to $\delta^{18}\text{O}$ values with reference to VSMOW by comparison with co-run IAEA-CH-3 cellulose (assuming $\delta^{18}\text{O} = +31.9 \pm 0.5\%$; Hunsinger et al., 2010). The within-run precision of IAEA-CH-3 $\delta^{18}\text{O}$ was $\leq 0.2\%$ (1 standard deviation). Standards were included at an interval of every eight samples. For the other species (*Tachigali*, *Amburana*, *Peltogyne*, *Bertholletia*, *Cedrelinga*, *Couratari* and *Polylepis*) $^{18}\text{O}/^{16}\text{O}$ ratios were measured in SEE at the University of Leeds, using continuous flow mass-spectrometry. Cellulose samples were thermally decomposed in an Elementar Vario Pyrocube in the absence of oxygen at 1450 °C, prior to analysis by an Isoprime continuous flow mass spectrometer. $^{18}\text{O}/^{16}\text{O}$ ratios were converted to $\delta^{18}\text{O}$ values versus VSMOW with reference to cellulose from Sigma-Aldrich, UK (Lot#SLBD2972V; for clarity hereafter referred to as Leeds Sigma cellulose). The Leeds Sigma cellulose was analysed at SEE against IAEA-CH-3

cellulose (assuming $\delta^{18}\text{O} = +31.9 \pm 0.5\%$; Hunsinger et al., 2010) and assigned a value of $29.2 \pm 0.2\%$. Standards were included at an interval of every twelve samples. The “reference” $\delta^{18}\text{O}_{\text{TR}}$ chronology from Brienen et al. (2012; hereafter referred to as *Cedrela*₂₀₁₂) was analysed at GFZ utilizing a “low” temperature pyrolysis (1.080 °C) in an element analyser (Carlo Erba) coupled to OPTIMA (Micromass Ltd., UK) IRMS. Two standards, IAEA-CH-3 and Merck cellulose (Darmstadt, Germany), were included at an interval of every eight samples. At the time, their $\delta^{18}\text{O}$ values were defined as $+32.6 \pm 0.3\%$ and $+28.7 \pm 0.3\%$ (Boettger et al., 2007). This method is no longer in use at GFZ. Currently, a ThermoFinnigan (Bremen, Germany) TC/EA set to 1400 °C, coupled to a Delta V Advantage IRMS is utilized. Re-analysis of IAEA-CH-3 and Merck cellulose resulted in $\delta^{18}\text{O}$ values of $+32.95 \pm 0.3\%$ and $+28.20 \pm 0.3\%$ respectively, after calibration against a different batch of Sigma-Aldrich cellulose (Lot#92F0243; $+27.3 \pm 0.3\%$, Boettger et al., 2007; Loader et al., 2014), IAEA-601 (benzoic acid; $\delta^{18}\text{O} = +23.15 \pm 0.3\%$) and IAEA-602 (benzoic acid; $\delta^{18}\text{O} = +71.28 \pm 0.5\%$; Brand et al., 2009). For an interlaboratory comparison

the Leeds Sigma-Aldrich cellulose was analysed at each of the labs, yielding the following values: $+29.1 \pm 0.2\%$ (NIGF; $n = 23$), $+29.2 \pm 0.2\%$ (SEE; $n = 20$), and $+30.2 \pm 0.35\%$ (GFZ; $n = 17$). Note that the ca. 1‰ offset between Leeds Sigma cellulose analysed at GFZ and the other two laboratories is consistent with the ca. 1‰ difference between the $\delta^{18}\text{O}$ values assigned to IAEA-CH-3. Hence the *Cedrela*₂₀₁₂ chronology measured at GFZ is likely to be offset by approximately 1‰ from the other datasets. However, we abstained from applying a correction to *Cedrela*₂₀₁₂ as interannual variance of $\delta^{18}\text{O}$ is of greater importance in this study than absolute values.

2.4. Dating calibration and radiocarbon verification

Exact dating of tree rings is a necessity for palaeoclimate reconstructions. In tree rings this is often done by matching ring-width patterns between dated and undated chronologies, also called cross-dating (Speer, 2010). Dating of tropical tree rings through this technique poses a particular challenge, as ring anatomy is often less clear in comparison with temperate trees, and regularly presents wedging (locally absent) or false rings (e.g. Priya and Bhat, 1998; Worbes, 2002). In addition, interannual variation in climate may not be the main driver of variation in growth, thus resulting in low common signals in ring-width, and poor cross-dating statistics (Brienen and Zuidema, 2005). Here we use a fresh approach to correct for dating errors, through cross-dating the isotope series from each species with an established isotope chronology. The method and approach are outlined below.

First we cross-dated tree rings using the standard ring-width approach: rings were marked and visually cross-dated across 2–4 radii on intact discs, ensuring every tenth ring interconnected between radii to detect errors. Rings were measured and a quality control was conducted using correlation analysis (programme COFECHA; Grissino-Mayer, 2001; Holmes, 1983). Ring-width series were detrended using a flexible cubic spline method, and a tree ring chronology was built with ARSTAN, only using series that passed the quality control. For several species inter-tree correlations were low ($r < 0.3$; Brienen and Zuidema, 2005), and they presented a varying degree of problems during cross-dating using standard ring-width. As a result, for most species only approximately half of the trees were incorporated in the ring-width chronologies. For full details see Brienen and Zuidema (2005).

Secondly, $\delta^{18}\text{O}_{\text{TR}}$ records developed in this study were aligned against the published *C. odorata* $\delta^{18}\text{O}_{\text{TR}}$ chronology from (Brienen et al., 2012; hereafter referred to as *Cedrela*₂₀₁₂). We initially performed a visual comparison, allowing the identification of tree ring sections where mistakes in the original dating could have been made due to missing rings or the inclusion of false rings. The original sample of wood was then re-inspected to see whether any rings had been missed (to support adding in a ring), or falsely identified (to support ring deletion from the series; see Table 3). Curves were only shifted if wood anatomical features in the original sample suggested false or wedging rings.

Finally, the dating of the newly aligned chronologies was verified using radiocarbon “bomb-peak” dating for species *Bertholletia*, *Couratari*, *Amburana*, *Peltogyne* and *Cedrelinga*. This methodology utilizes the near doubling of atmospheric ^{14}C during the nuclear tests of the 1960s to date modern organic material (Worbes and Junk, 1989). Cellulose extracted from the rings dated as 1975 (using the isotope cross-dating approach described above) were analysed in Bothell, USA by DirectAMS. The ^{14}C concentrations were normalized to a value of $\delta^{13}\text{C} = -25\%$ to correct for isotopic fractionation. The SHCal13 radiocarbon calibration curve from Hogg et al. (2013) was used alongside the bomb extension curve from Hua et al. (2013) to convert pMC (percent Modern Carbon) values to actual calendar dates using the free online CALIBomb software (<http://calib.qub.ac.uk>). Calendar dates were assigned to rings according to the year in which the growth

started. Thus, the ring spanning calendar years 1975 to 1976 is here called 1975.

2.5. Statistical analysis

Using the $\delta^{18}\text{O}_{\text{TR}}$ data from the nine *Cedrela* trees, we constructed an isotope chronology for the period 1901–2001 (hereafter referred to as *Cedrela*₂₀₁₅). The minimum number of samples at any point along the chronology is three. “Expressed Population Signal” (EPS) was calculated according to Wigley et al. (1984), using the formula $(N * r_{\text{mean}}) / (1 + (N - 1) * r_{\text{mean}})$, where N is the number of time series and r_{mean} is the mean inter-series correlation coefficient. An EPS threshold of 0.85 is generally used to determine whether individual tree-level (<0.85) or stand-level (>0.85) signals dominate a chronology (Wigley et al., 1984). We correlated the *Cedrela*₂₀₁₅ chronology with the *Cedrela*₂₀₁₂ chronology, and the different species’ records were correlated with either *Cedrela*₂₀₁₂ or *Cedrela*₂₀₁₅, depending on which was geographically closest to the sample site of that species. The *Polylepis* series was also compared with the Navado Sajama ice-core record (data extracted from Hardy et al., 2003), and the published *Polylepis* $\delta^{18}\text{O}_{\text{TR}}$ chronology from Ballantyne et al. (2011). All correlations used the “Pearson’s product–moment correlation” method and were calculated in the statistical programme *R* (R Development Core Team, 2015). This method uses the formula $r_{XY} = (\text{cov}(X,Y)) / (\sigma_X \sigma_Y)$ where r_{XY} is the correlation coefficient, cov is the covariance and σ_X and σ_Y are the standard deviations of the time series X and Y respectively. To visualize decadal trends, a second order, low-pass Butterworth filter with a cut-off frequency of 0.2 was applied in both the forward and reverse directions for each series, using the *R* package “signal” (Ligges et al., 2015).

3. Results and discussion

3.1. Cross-dating tree ring oxygen isotope series

Radiocarbon dating proves that $\delta^{18}\text{O}$ can be used to date tree rings more accurately than simple ring counting (Table 2). For three out of the five species tested for radiocarbon (*Couratari*, *Amburana*, and *Cedrelinga*) the $\delta^{18}\text{O}_{\text{TR}}$ -adjusted ring dates match the radiocarbon age estimates. For these species mistakes made during the initial ring counting were correctly identified through comparison of their $\delta^{18}\text{O}_{\text{TR}}$ -series with the *Cedrela*₂₀₁₂ reference chronology. The validation of this technique is an important result, since it shows that $\delta^{18}\text{O}_{\text{TR}}$ can help with the detection of false or missing rings, potentially offering a simple way to correct for minor dating inaccuracies. The ability to precisely cross-date $\delta^{18}\text{O}_{\text{TR}}$ series over different sites and species could also facilitate the construction of new chronologies. A similar method was used to date dead tropical wood through cross-dating high-resolution $\delta^{13}\text{C}$ series with precipitation records (Fichtler et al., 2010), and other tropical studies have highlighted the utility of high-resolution isotope measurements in cases where ring detection is difficult (e.g. Boysen et al., 2014; Pons and Helle, 2011) or rings are not visible at all (e.g. Anchukaitis and Evans, 2010; Poussart et al., 2004). In a comparison of pine and oak $\delta^{18}\text{O}_{\text{TR}}$ from Japan, Li et al. (2015) suggest that oxygen isotopes can also be used to cross-date between angiosperm and gymnosperm species. Nevertheless, cross-dating interannual $\delta^{18}\text{O}_{\text{TR}}$ variability with an established chronology for dating verification has not, to the best of our knowledge, been previously applied in a tropical context.

For all species, except *Tachigali* and *Polylepis*, our analysis indicates that rings must have been missed during the initial ring counting based purely on macroscopical wood anatomy (i.e., before comparison of the oxygen isotope series with the reference chronology, see Table 3). The exact number of rings missed in the *Bertholletia* record is unknown, although radiocarbon dating suggests a disparity of 1–4 years up to 1975. It was not possible to use $\delta^{18}\text{O}_{\text{TR}}$ to correct the dating of *Bertholletia* or *Peltogyne*, as these species showed a low degree of

Table 2

Radiocarbon “bomb-peak” dating results. Calendar dates were assigned to tree rings according to the year in which the growth started. Thus a ring may be correctly dated if the radiocarbon age estimate encompasses the $\delta^{18}\text{O}_{\text{TR}}$ -adjusted age estimate plus one year. Percent Modern Carbon (pMC) values were converted to calendar dates using the free online CALIBomb software (<http://calib.qub.ac.uk>).

| Species | $\delta^{13}\text{C}$ | pMC | 1 σ error | Ring counting age estimate | $\delta^{18}\text{O}_{\text{TR}}$ -adjusted age estimate | Radiocarbon age (1 SD) | Radiocarbon age (2 SD) | Correctly dated? |
|---------------------|-----------------------|--------|------------------|----------------------------|----------------------------------------------------------|------------------------|------------------------|------------------|
| <i>Couratari</i> | 22.9 | 134.73 | 0.37 | 1979 | 1975 | 1976.5–1977 | 1976–1978 | Yes |
| <i>Amburana</i> | 21.2 | 135.16 | 0.36 | 1979 | 1975 | 1976–1977 | 1975.5–1978 | Yes |
| <i>Cedrelinga</i> | 20.5 | 136.81 | 0.37 | 1978 | 1975 | 1975.5–1976.5 | 1974.5–1976.5 | Yes |
| <i>Bertholletia</i> | 23.0 | 146.51 | 0.38 | 1975 | 1975 | 1973 | 1972.5–1974 | 1–4 years out |
| <i>Peltogyne</i> | 21.6 | 159.81 | 0.42 | 1975 | 1975 | 1964 or 1967 | 1964 or 1967–8 | 7–12 years out |

synchronicity with the reference isotope curve making curve fitting impossible. Of all the species *Peltogyne* and *Couratari* had the highest number of dating errors, as revealed by radiocarbon dating (Table 3). For *Peltogyne* 13 rings were missed in the outermost part of the sample, the sapwood, where rings are markedly less distinct (Brienen and Zuidema, 2005), while for *Couratari* eight rings were identified which had been missed during the original mark-up, predominantly in sections with reduced ring visibility, or where rings were very narrow. Additional mistakes arose due to misidentification of resin bands as rings, particularly in *Cedrela*, a species that is known to form non-annual resin bands (Dünisch et al., 2002). These problems in ring dating using only standard, anatomical ring detection methods confirm the continuing challenges in tropical tree ring analysis (Groenendijk et al., 2014; Stahle, 1999).

3.2. *Cedrela* chronology

The nine *Cedrela* trees from Selva Negra show high synchronicity in their $\delta^{18}\text{O}_{\text{TR}}$ (Fig. 2; mean inter-tree correlation (r_{mean}) for 1901–2001 = 0.71), and a high “Expressed Population Signal” (EPS; Wigley et al., 1984) of 0.96, suggesting that $\delta^{18}\text{O}_{\text{TR}}$ is dominated by a strong external control. These values are highly comparable with the results of *Cedrela*₂₀₁₂ (Brienen et al., 2012; r_{mean} = 0.63, EPS = 0.97, 1900–2001), and suggest similar drivers to the *Cedrela*₂₀₁₂ chronology, i.e. $\delta^{18}\text{O}_{\text{P}}$ (Brienen et al. 2012). It indicates that *Cedrela* is a well-suited species for reconstructing $\delta^{18}\text{O}_{\text{P}}$. *Cedrela* trees are shallow-rooted and favour sites with good drainage (Cintron 1990), using water from the top 30 cm of the soil profile (Schwendenmann et al., 2014). We thus expect $\delta^{18}\text{O}_{\text{TR}}$ of *Cedrela* to predominantly reflect the isotopic composition

Table 3

Dating corrections applied following verification process. Columns indicate the number of rings that were inserted or deleted based on comparison of the respective $\delta^{18}\text{O}_{\text{TR}}$ series with the reference *Cedrela*₂₀₁₂ $\delta^{18}\text{O}_{\text{TR}}$ chronology, or corrections made due to radiocarbon dating methods (only for *Peltogyne*). The mistake rate was calculated by dividing the number of corrected rings by the length of the series.

| Species | Record period | Dating with $\delta^{18}\text{O}_{\text{TR}}$ | | Radiocarbon dating | | Mistake rate |
|---------------------|---------------|-----------------------------------------------|---------------|--------------------|---------------|--------------|
| | | Rings inserted | Rings deleted | Rings inserted | Rings deleted | |
| <i>Cedrela</i> | | | | | | |
| Tree 11 | 1920–2010 | 1 | 3 | – | – | 0.0444 |
| Tree 12 | 1941–2010 | 0 | 0 | – | – | 0 |
| Tree 13 | 1915–2010 | 2 | 1 | – | – | 0.0316 |
| Tree 14 | 1908–2010 | 0 | 3 | – | – | 0.0294 |
| Tree 16 | 1884–2010 | 0 | 0 | – | – | 0 |
| Tree 20 | 1904–2010 | 4 | 3 | – | – | 0.0660 |
| Tree 21 | 1898–2010 | 0 | 1 | – | – | 0.00893 |
| Tree 23 | 1897–2010 | 8 | 1 | – | – | 0.0796 |
| Tree 27 | 1903–2010 | 0 | 0 | – | – | 0 |
| <i>Tachigali</i> | 1990–2002 | 0 | 0 | – | – | 0 |
| <i>Amburana</i> | 1897–2000 | 2 | 0 | 0 | 0 | 0.0194 |
| <i>Couratari</i> | 1892–2008 | 8 | 0 | 0 | 0 | 0.0690 |
| <i>Peltogyne</i> | 1929–1990 | – | – | 13 | 0 | 0.2131 |
| <i>Cedrelinga</i> | 1950–1999 | 3 | 0 | 0 | 0 | 0.0612 |
| <i>Bertholletia</i> | 1896–2001 | – | – | – | – | ? |
| <i>Polylepis</i> | 1931–2002 | 0 | 0 | – | – | 0 |

of recent rainfall, and be only minimally influenced by groundwater, which could potentially dampen the interannual variability of the chronology.

In contrast to $\delta^{18}\text{O}_{\text{TR}}$, inter-tree correlation and EPS for tree ring-width were much lower for the nine *Cedrela*₂₀₁₅ trees (r_{mean} = 0.17, EPS = 0.64). This has been found for other tree species across the tropics. For example, *Fokienia hodginsii* in Laos (Xu et al., 2011), *Entandrophragma utile* in Cameroon (van der Sleen et al., 2015) and *Mimosa acantholoba* in Mexico (Brienen et al., 2013) all show better coherence in $\delta^{18}\text{O}_{\text{TR}}$ than in growth. These studies show that in the tropics $\delta^{18}\text{O}_{\text{TR}}$ is often more sensitive than ring-width to external climate forcings, and therefore makes a better climate proxy. One exception is *Tectona grandis* (teak) in Indonesia, where inter-tree synchronization in $\delta^{18}\text{O}_{\text{TR}}$ and ring-width are more comparable (e.g. Poussart et al., 2004; Schollaen et al., 2013).

Given the high cost of isotope measurements it is of interest to quantify the minimum number of trees needed to establish a robust $\delta^{18}\text{O}_{\text{TR}}$ chronology. An EPS above 0.85 has been suggested to imply good internal coherence, with the minimum number of cores needed to exceed this threshold dependent on the strength of the common signal (i.e. when the inter-series correlation is low, more cores are required to build a satisfactory chronology; Wigley et al., 1984). The results of *Cedrela*₂₀₁₅ imply that this threshold would have been exceeded with just three trees when using $\delta^{18}\text{O}_{\text{TR}}$. In contrast, to create a standard ring-width chronology approximately 28 trees would have been required to reach an EPS of 0.85 (see Cook and Kairiukstis, 1990).

3.3. Inter-specific coherence in tree ring oxygen isotopes

The $\delta^{18}\text{O}_{\text{TR}}$ records of five of the six lowland species showed significant correlations with the closest *Cedrela* $\delta^{18}\text{O}_{\text{TR}}$ chronology (Fig. 3). Only *Bertholletia* showed no significant relationship ($r = -0.15$, $p = 0.14$, 1901–2001). Although the *Tachigali* series only spans a short period (13 years), it showed the strongest relationship with *Cedrela*₂₀₁₅ ($r = 0.90$, $p < 0.001$, 1990–2001), approximately 100 km away. *Peltogyne* also correlated quite well with *Cedrela*₂₀₁₅ ($r = 0.39$, $p < 0.01$, 1929–1990), but had a stronger relationship with the *Cedrela*₂₀₁₂ curve from the more distant Purissima site ($r = 0.58$, $p < 0.001$, 1929–1990, not shown). *Amburana* also correlated well with *Cedrela*₂₀₁₂ from the same location ($r = 0.41$, $p < 0.001$, 1901–2000). The relationship between *Cedrelinga* and *Cedrela*₂₀₁₅ was slightly weaker ($r = 0.33$, $p < 0.05$, 1950–1999), as was the correlation between *Couratari* and *Cedrela*₂₀₁₅ ($r = 0.27$, $p < 0.05$, 1901–2001). These close inter-species relationships most likely arise from a dominant imprint of interannual variation in $\delta^{18}\text{O}_{\text{P}}$ on $\delta^{18}\text{O}_{\text{TR}}$, via a strong influence of $\delta^{18}\text{O}_{\text{S}}$.

Correlations between the different lowland tree species were also evaluated. *Bertholletia* was excluded from the analysis due to the uncertainties with regard to its dating precision. The mean inter-species correlation coefficient for six species including *Cedrela*₂₀₁₅ is 0.37. This value is slightly higher than that found by Saurer et al. (2008) for trees in a temperate region (r_{mean} = 0.23), comparing records from sites with smaller distances between them (<160 km vs. <325 km in this study). The observed difference in correlations between these studies can possibly be explained by higher levels of precipitation during the

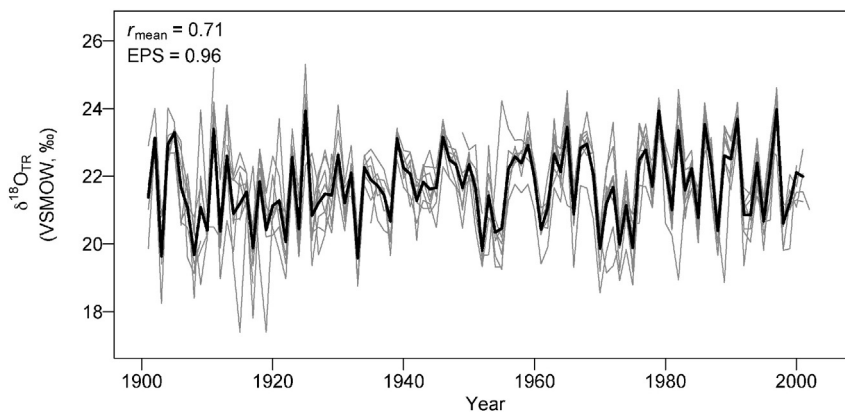


Fig. 2. Interannual variation in $\delta^{18}\text{O}_{\text{TR}}$ in nine *Cedrela odorata* trees from Selva Negra, Bolivia (grey lines), and the mean $\delta^{18}\text{O}_{\text{TR}}$ chronology (black line) from 1901 to 2001. The mean inter-tree correlation for the period 1901–2001 is 0.71 and the Expressed Population Signal (EPS) is 0.96, calculated according to Wigley et al. (1984).

growing season for our Amazon site compared to the temperate study, thus reducing the influence of residual soil water which may dampen variation in $\delta^{18}\text{O}_s$ (Treydte et al., 2014). In addition, the sites in the Saurer et al. (2008) study are situated in a heterogeneous mountainous environment with varying altitudes (480–1400 m.a.s.l.), and as $\delta^{18}\text{O}_p$ varies strongly with altitude (Dansgaard, 1964), this may explain the lower correspondence between their trees.

Despite showing similar trends in $\delta^{18}\text{O}_{\text{TR}}$, we observed a degree of variation between the isotope series for the different species. The two most likely causes for this variation are differences in partitioning of water sources between species, and species-specific differences in plant physiology. Differences in partitioning of water sources arise due to differences in rooting structure/depth (spatial partitioning) or due to differences between species' growing season, or timing of wood formation (temporal partitioning). Rooting depth affects $\delta^{18}\text{O}_s$ due to the existence of isotopic gradients in soil water. These arise from surface evaporation enriching the isotope signal at the surface, and mixing of precipitation with residual pools of groundwater in lower soil layers (Ehleringer and Dawson, 1992; Tang and Feng, 2001). While model simulation experiments suggest that the influence of soil evaporation on $\delta^{18}\text{O}_{\text{TR}}$ is likely to be minimal in the Amazon Basin (Kanner et al., 2014), xylem water $\delta^{18}\text{O}$ of tropical trees in Panama show inter-species variation up to 7‰, reflecting downward isotopic gradients in soil water, and differences between species in water uptake depth (Schwendenmann et al., 2014). For our species little is known about the rooting depth (Table 1), but differences in phenology may provide some indication: Retention of leaves during the dry season could indicate that trees have access to deeper groundwater (Borchert, 1994; Jackson et al., 1995; Schwendenmann et al., 2014), and water uptake from deeper soil layers during this dry period may affect the interannual $\delta^{18}\text{O}$ signal recorded in cellulose. For example *Cedrelinga*, which is brevi-deciduous with a gradual turnover of leaves at the end of the dry season (Brienen and Zuidema, 2005), showed only a weak correlation with *Cedrela*.

In addition to spatial partitioning of source water, species may also vary in timing of their water uptake and wood formation through the year. This temporal partitioning may be as important as spatial partitioning, since seasonal variation in $\delta^{18}\text{O}_p$ is large in Bolivia (i.e. approx. 9‰, GNIP data; see also Brienen et al., 2012), and studies elsewhere have shown that such variability can be reflected in $\delta^{18}\text{O}_{\text{TR}}$ (e.g. Schollaen et al., 2013). Differences in timing of water uptake and wood formation could mean species record $\delta^{18}\text{O}_p$ over slightly different timeframes. *Amburana* and *Cedrela* are strictly deciduous, with defoliation occurring from July to October for both species (Brienen and Zuidema, 2005). These species are therefore likely to use water during the same period in the year, possibly causing the good correspondence between their $\delta^{18}\text{O}_{\text{TR}}$ records. *Bertholletia*, another deciduous species, showed no relationship with the *Cedrela* $\delta^{18}\text{O}_{\text{TR}}$ record at interannual

or decadal timescales, but this may be because it retains its leaves well into the start of the dry season, suggesting it may grow for longer and use water from the start of the dry season. This could also be true for the other brevi-deciduous species, which never appear completely leafless for extended periods (see Table 1).

Differences in plant physiology may also explain some of the variability seen between $\delta^{18}\text{O}_{\text{TR}}$ records. For example, “effective path length” (the pathway of water movement through the leaf to the site of evaporation and an important determinant of the Péclet effect), has been found to drive variation in $\delta^{18}\text{O}_L$ within and between species (e.g. Kahmen et al., 2008; Song et al., 2013). In addition, interspecific variation in transpiration rates and transpiration responses to changes in relative humidity (RH) may affect the degree to which variation in $\delta^{18}\text{O}_s$ is maintained in $\delta^{18}\text{O}_{\text{TR}}$ for the different species. For example, leaf water enrichment may have a relatively greater influence on $\delta^{18}\text{O}_{\text{TR}}$ than source water influences for those species with generally lower transpiration rates, or for species whose growing season extends into the dry season when RH is expected to be lower. This may be another reason why *Bertholletia* shows no correlation with *Cedrela* $\delta^{18}\text{O}_{\text{TR}}$. However, exchange of oxygen atoms between cellulose-precursors and non-enriched stem water during phloem loading (Gessler et al., 2013) and/or cellulose synthesis (Hill et al., 1995; Song et al., 2013) reinforces the signature of source water on $\delta^{18}\text{O}_{\text{TR}}$ such that short term variation in $\delta^{18}\text{O}_L$ may not be reflected in the final $\delta^{18}\text{O}_{\text{TR}}$ signal (Treydte et al., 2014). The extent of exchange may vary between species, and is thought to explain why oak $\delta^{18}\text{O}_{\text{TR}}$ records from Japan showed lower sensitivity to changes in RH than pine $\delta^{18}\text{O}_{\text{TR}}$ records (Li et al., 2015). The degree of exchange is positively related to the time between carbohydrate production in the leaf and cellulose synthesis in the stem (i.e. the turnover time of carbohydrates, Song et al., 2014b), which may itself vary considerably between species. These physiological processes may all contribute, in part, to the variation observed between $\delta^{18}\text{O}_{\text{TR}}$ records in this study.

3.4. Spatial coherence of oxygen isotopes in tree rings

Despite the considerable distance between sites (approx. 325 km), there is a strong correlation between the *Cedrela*₂₀₁₅ chronology and the published *Cedrela*₂₀₁₂ record (Brienen et al., 2012; Fig. 4; $r = 0.80$, $p < 0.001$, 1901–2001). This suggests that factors influencing $\delta^{18}\text{O}_{\text{TR}}$ in this part of the Amazon Basin are acting at a large scale. Poussart et al. (2004) also report synchronization of $\delta^{18}\text{O}_{\text{TR}}$ in two *Samanea saman* trees thought to be from different forests in Java, Indonesia, although the precise origins of the trees are unknown. A strong correlation between $\delta^{18}\text{O}_{\text{TR}}$ records from relatively distant sites can arise from either a strong source water signal, or spatially coherent changes in RH influencing transpiration and thus the Péclet number and $\delta^{18}\text{O}_L$ (see Section 1). Since RH depends on local climate conditions and may thus

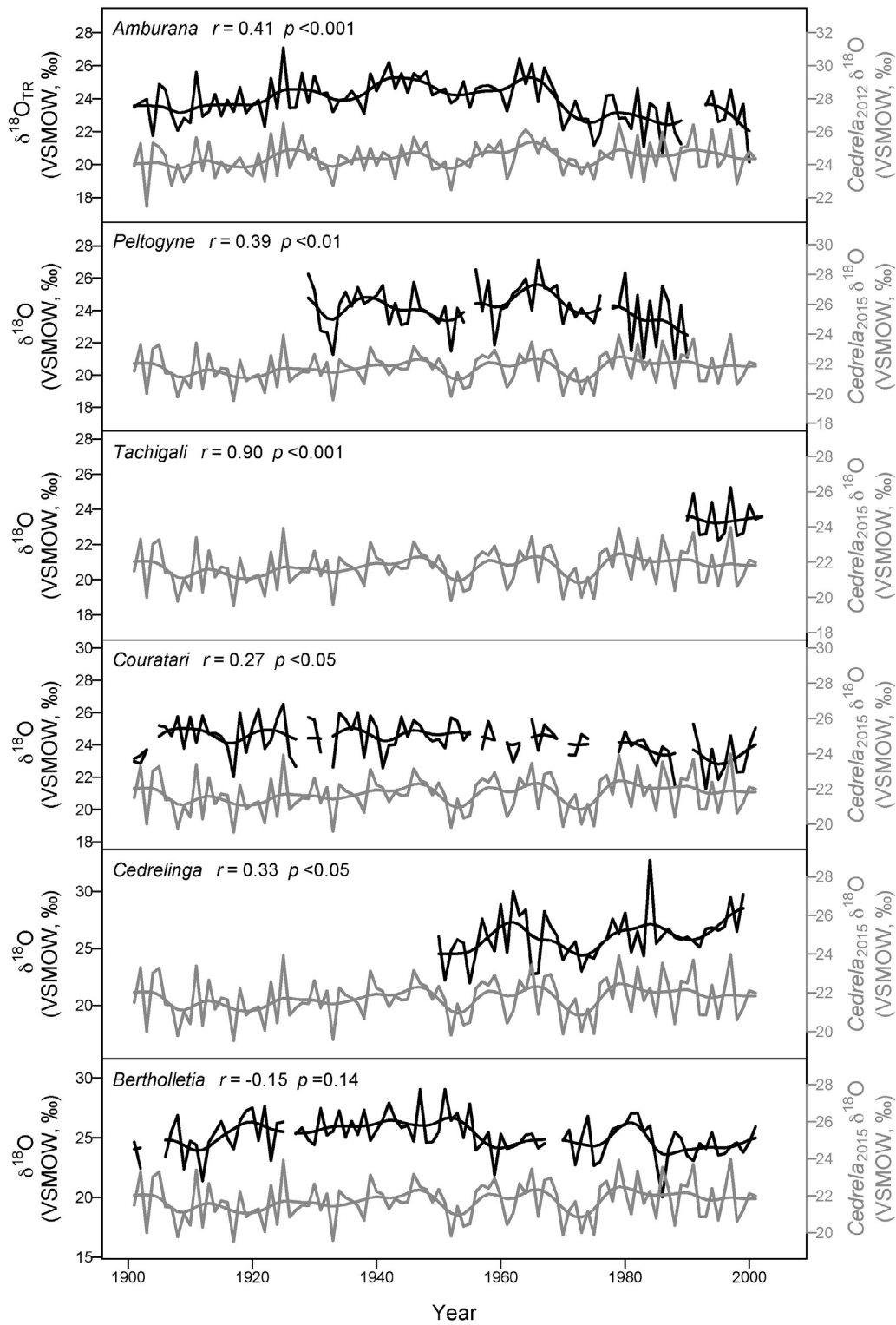


Fig. 3. $\delta^{18}\text{O}_{\text{TR}}$ time series for six tropical tree species (black lines) and *Cedrela* $\delta^{18}\text{O}_{\text{TR}}$ (grey lines). Pearson correlation coefficients and significance levels are shown at the top of each panel. In some cases records are discontinuous because of insufficient sample material for isotope analysis in years with very narrow rings. A low-pass Butterworth filter was applied to each series to visualize decadal variation.

vary over short distances, we expect that the common interannual variation between the two chronologies is mostly driven by a dominant source water influence on $\delta^{18}\text{O}_{\text{TR}}$. Assuming that plant source water is predominantly recent precipitation, as opposed for example to groundwater, the strong coherence between these *Cedrela* records also reveals that $\delta^{18}\text{O}_{\text{P}}$ is itself coherent over wide areas. Thus $\delta^{18}\text{O}_{\text{P}}$ in the study region is primarily controlled by large-scale processes, such as Rayleigh

rainout (continental effect) and evaporative recycling during moisture transport to the site of precipitation, rather than a local amount effect (Dansgaard, 1964; Rozanski et al., 1993; Salati et al., 1979). This was previously suggested by Brienen et al. (2012) based on comparisons of $\delta^{18}\text{O}_{\text{TR}}$ with $\delta^{18}\text{O}_{\text{P}}$ records from the basin (from the Global Network of Isotopes in Precipitation, GNIP), and with local and basin-wide climate.

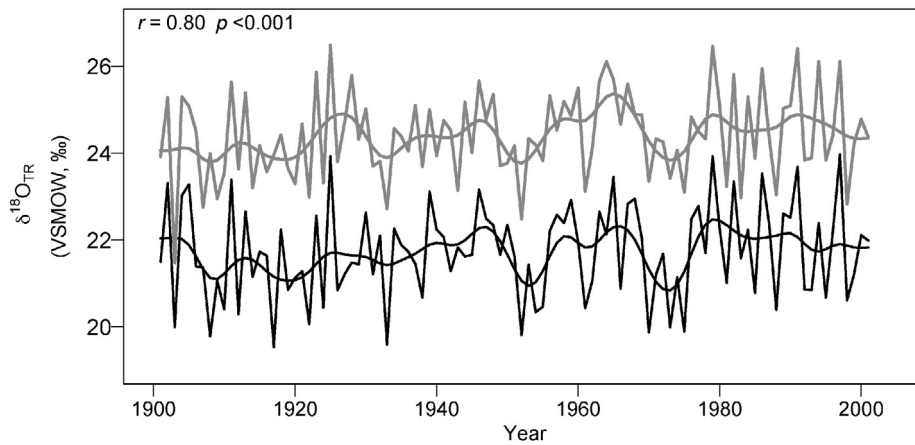


Fig. 4. Interannual variation in $\delta^{18}\text{O}_{\text{TR}}$ in the *Cedrela*₂₀₁₅ chronology from Selva Negra, Bolivia (black), and in the *Cedrela*₂₀₁₂ chronology from Purisima, Bolivia (grey; record from Brienen et al., 2012). The Pearson correlation coefficient is 0.80 for the full period, 1901–2001. A low-pass Butterworth filter was applied to each series to visualize decadal variation.

Further support for spatial coherence in $\delta^{18}\text{O}_{\text{TR}}$ comes from a comparison of the Altiplano *Polylepis* record and the lowland *Cedrela*₂₀₁₅ chronology. The correlation between these two records is significant, but much weaker than the correlation between the two lowland *Cedrela* chronologies (i.e. $r = 0.39$, $p < 0.01$, 1931–2001, not shown). A weaker correlation is expected for several reasons: Firstly, the two records are simply further apart (approx. 1000 km). Secondly, *Polylepis* grows in the Altiplano, a very dry plateau with an average height of approximately 3800 m, and the factors controlling $\delta^{18}\text{O}_{\text{TR}}$ are likely to differ between the lowland and the highland trees. Thirdly, while the dominant source of moisture for the Altiplano is the Amazon Basin (Garreaud, 2000), orographic precipitation as air masses rise over the foothills of the Andes will increase the rainout of heavy isotopes (altitude effect; Dansgaard, 1964; Grootes et al., 1989; Rozanski et al., 1993), and subsequent transport of moisture over approximately 200 km of dry, high-altitude desert will further alter Altiplano $\delta^{18}\text{O}_{\text{P}}$ in comparison with the Amazon. These additional alterations to the $\delta^{18}\text{O}$ signal of moisture originating from the Amazon probably explain the greater variability in the Altiplano series (i.e. standard deviation for *Polylepis* = 2.3‰ vs. 1.07‰ for *Cedrela*). The *Polylepis* series was also found to correlate with two other Altiplano isotope series: The nearby Nevado Sajama ice-core $\delta^{18}\text{O}$ record ($r = 0.44$, $p < 0.001$, 1948–1996; Fig. 5) and a *Polylepis* $\delta^{18}\text{O}_{\text{TR}}$ record from Volcan Granada, Argentina, approximately 500 km south ($r = 0.30$, $p < 0.05$, not shown; Ballantyne et al., 2011). This suggests that $\delta^{18}\text{O}_{\text{P}}$ retains a reasonable degree of coherence over the plateau. The spatial

coherence of $\delta^{18}\text{O}$ records from distant sites provides further evidence for a broad common signal in $\delta^{18}\text{O}_{\text{P}}$, extending from the basin to the Altiplano, and confirms the interpretation of highland $\delta^{18}\text{O}$ records such as ice cores as, at least partially, a record of precipitation over the Amazon Basin (Brienen et al., 2012; Hoffmann, 2003).

4. Conclusions

Comparison of $\delta^{18}\text{O}_{\text{TR}}$ series from eight tropical tree species from four sites ranging from lowland rainforest to the Bolivian Altiplano showed that $\delta^{18}\text{O}_{\text{TR}}$ can be used to cross-date tree ring chronologies from the tropics with higher accuracy than simple ring-width measurements. Six of the seven lowland species analysed show matching interannual variation in $\delta^{18}\text{O}_{\text{TR}}$, suggesting they all preserve variation in source water isotopic composition. We found that $\delta^{18}\text{O}_{\text{TR}}$ records correlated well over large distances (< 1000 km), which suggests a dominant influence of source water on the cellulose signal, and that $\delta^{18}\text{O}_{\text{P}}$ in this region is similar over large spatial scales. The coherent imprint of $\delta^{18}\text{O}_{\text{TR}}$ across different species and sites has important implications for future studies in the Amazon, offering the potential to reconstruct $\delta^{18}\text{O}_{\text{P}}$, and thus rainfall over a large and globally important area. In context of the recent hydrological intensification (Gloor et al., 2013) and uncertainties about the direction of future precipitation changes in the Amazon (Zhang et al., 2015), development of a network of extended

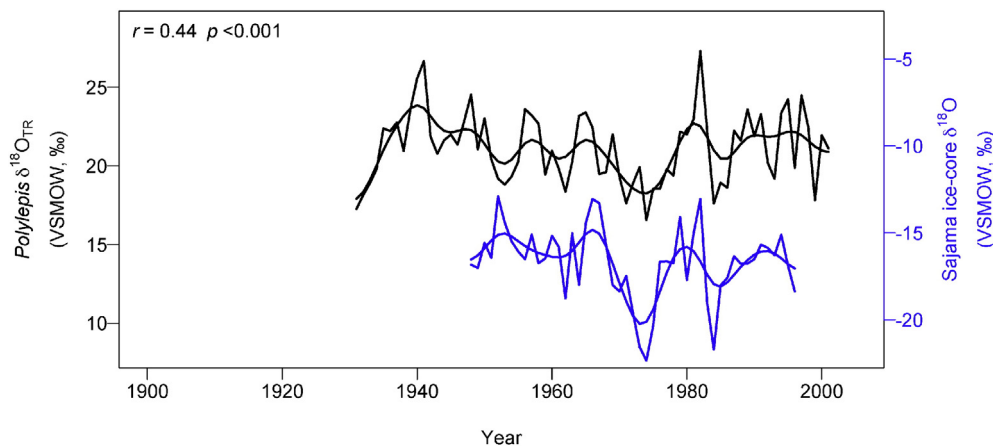


Fig. 5. *Polylepis* $\delta^{18}\text{O}_{\text{TR}}$ record (black) and the Sajama ice-core $\delta^{18}\text{O}$ record (blue). The Pearson correlation coefficient is 0.44 for the period 1948–1996. A low-pass Butterworth filter was applied to each series to visualize decadal variation. (For interpretation of the references to color in this figure legend, the reader is referred to the online version of this chapter.)

$\delta^{18}\text{O}_{\text{TR}}$ records across the Amazon would be a significant step towards a better understanding of the region's complex hydrology.

Acknowledgements

We thank Vincent Vos, Guido Pardo, Don Nico Divico and Nazareno Martinez for their help with the fieldwork in Pando, Bolivia in 2011 and logistic planning. This work has been supported principally by the Natural Environmental Research Council through a NERC Research Fellowship to RJWB (grant NE/L021160/1), NERC standard grant (NE/K01353X/1), and by NERC Isotope Geosciences Facilities grants (IP-1424-0514 and IP-1314-0512). JCAB is funded by a NERC Doctoral Training Grant (NE/L501542/1).

References

- Anchukaitis, K.J., Evans, M.N., 2010. Tropical cloud forest climate variability and the demise of the Monteverde golden toad. *Proc. Natl. Acad. Sci.* 107 (11), 5036–5040.
- Argollo, J., Soliz, C., Villalba, R., 2004. Potencialidad dendrocronológica de *Polylepis tarapacana* en los Andes Centrales de Bolivia. *Ecol. Bolivia* 39 (1), 1–24.
- Ballantyne, A., Baker, P., Chambers, J., Villalba, R., Argollo, J., 2011. Regional differences in South American Monsoon precipitation inferred from the growth and isotopic composition of tropical trees. *Earth Interact.* 15 (5), 1–35.
- Barbour, M.M., Roden, J.S., Farquhar, G.D., Ehleringer, J.R., 2004. Expressing leaf water and cellulose oxygen isotope ratios as enrichment above source water reveals evidence of a Péclet effect. *Oecologia* 138 (3), 426–435.
- Boettger, T., et al., 2007. Wood cellulose preparation methods and mass spectrometric analyses of $\delta^{13}\text{C}$, $\delta^{18}\text{O}$, and nonexchangeable $\delta^2\text{H}$ values in cellulose, sugar, and starch: an interlaboratory comparison. *Anal. Chem.* 79 (12), 4603–4612.
- Borchert, R., 1994. Soil and stem water storage determine phenology and distribution of tropical dry forest trees. *Ecology* 75 (5), 1437–1449.
- Boysen, B.M.M., Evans, M.N., Baker, P.J., 2014. $\delta^{18}\text{O}$ in the tropical conifer *Agathis robusta* records ENSO-related precipitation variations. *PLoS One* 9 (7), 9.
- Brand, W.A., et al., 2009. Comprehensive inter-laboratory calibration of reference materials for $\delta^{18}\text{O}$ versus VSMOW using various on-line high-temperature conversion techniques. *Rapid Commun. Mass Spectrom.* 23 (7), 999–1019.
- Brienen, R.J.W., Zuidema, P.A., 2005. Relating tree growth to rainfall in Bolivian rain forests: a test for six species using tree ring analysis. *Oecologia* 146 (1), 1–12.
- Brienen, R.J.W., Zuidema, P.A., 2006. Lifetime growth patterns and ages of Bolivian rain forest trees obtained by tree ring analysis. *J. Ecol.* 94 (2), 481–493.
- Brienen, R.J.W., Helle, G., Pons, T.L., Guyot, J.L., Gloor, M., 2012. Oxygen isotopes in tree rings are a good proxy for amazon precipitation and El Niño–Southern Oscillation variability. *Proc. Natl. Acad. Sci.* 109 (42), 16957–16962.
- Brienen, R.J.W., Hietz, P., Wanek, W., Gloor, M., 2013. Oxygen isotopes in tree rings record variation in precipitation $\delta^{18}\text{O}$ and amount effects in the south of Mexico. *J. Geophys. Res. Biogeosci.* 118 (4), 1604–1615.
- Briffa, K.R., 1999. Interpreting high-resolution proxy climate data – the example of dendroclimatology. *analysis of climate variability*. Springer, pp. 77–94.
- Cintron, B.B., 1990. *Cedrela odorata* L. Cedro hembra, Spanish cedar. 2(654), 250.
- Cook, E.R., Kairiukstis, L.A., 1990. *Methods of Dendrochronology: Applications in the Environmental Sciences*. Springer Science & Business Media.
- Dansgaard, W., 1964. Stable isotopes in precipitation. *Tellus* 16 (4), 436–468.
- Domic, A.I., Capriles, J.M., 2009. Allometry and effects of extreme elevation on growth velocity of the Andean tree *Polylepis tarapacana* Philippi (Rosaceae). *Plant Ecol.* 205 (2), 223–234.
- Dünisch, O., Bauch, J., Gasparotto, L., 2002. Formation of increment zones and intraannual growth dynamics in the xylem of *Swietenia macrophylla*, *Carapa guianensis*, and *Cedrela odorata* (Meliaceae). *IAWA J.* 23 (2), 101–120.
- Ehleringer, J., Dawson, T., 1992. Water uptake by plants: perspectives from stable isotope composition. *Plant Cell Environ.* 15 (9), 1073–1082.
- Farquhar, G., Lloyd, J., 1993. Carbon and oxygen isotope effects in the exchange of carbon dioxide between terrestrial plants and the atmosphere. *Stable Isotopes and Plant Carbon–Water Relations* 40, pp. 47–70.
- Fichtler, E., Helle, G., Worbes, M., 2010. Stable-carbon isotope time series from tropical tree rings indicate a precipitation signal. *Tree Ring Res.* 66 (1), 35–49.
- Garreaud, R., 2000. Intraseasonal variability of moisture and rainfall over the South American Altiplano. *Mon. Weather Rev.* 128 (9), 3337–3346.
- Gessler, A., et al., 2013. The oxygen isotope enrichment of leaf-exported assimilates – does it always reflect lamina leaf water enrichment? *New Phytol.* 200 (1), 144–157.
- Gloor, M., et al., 2013. Intensification of the amazon hydrological cycle over the last two decades. *Geophys. Res. Lett.* 40 (9), 1729–1733.
- Grissino-Mayer, H.D., 2001. Evaluating crossdating accuracy: a manual and tutorial for the computer program COFECHA. *Tree Ring Res.*
- Grissino-Mayer, H.D., Fritts, H.C., 1997. The International Tree-Ring Data Bank: an enhanced global database serving the global scientific community. *The Holocene* 7 (2), 235–238.
- Groenendijk, P., Sass-Klaassen, U., Bongers, F., Zuidema, P.A., 2014. Potential of tree-ring analysis in a wet tropical forest: a case study on 22 commercial tree species in Central Africa. *For. Ecol. Manag.* 323, 65–78.
- Grootes, P., Stuiver, M., Thompson, L., Mosley-Thompson, E., 1989. Oxygen isotope changes in tropical ice, Quelccaya, Peru. *J. Geophys. Res. Atmos.* 94 (D1), 1187–1194.
- Hardy, D., Vuille, M., Bradley, R., 2003. Variability of snow accumulation and isotopic composition on Nevado Sajama, Bolivia. *J. Geophys. Res. Atmos.* 108 (D22).
- Hill, S., Waterhouse, J., Field, E., Switzer, V., Ap Rees, T., 1995. Rapid recycling of triose phosphates in oak stem tissue. *Plant Cell Environ.* 18 (8), 931–936.
- Hoffmann, G., 2003. Coherent isotope history of Andean ice cores over the last century. *Geophys. Res. Lett.* 30 (4).
- Hogg, A.G., et al., 2013. SHCal13 Southern Hemisphere calibration, 0–50,000 years cal BP. *Radiocarbon* 55 (4), 1889–1903.
- Holmes, R.L., 1983. Computer-assisted quality control in tree-ring dating and measurement. *Tree-Ring Bull.* 43 (1), 69–78.
- Hua, Q., Barbetti, M., Rakowski, A.Z., 2013. Atmospheric radiocarbon for the period 1950–2010. *Radiocarbon* 55 (4), 2059–2072.
- Hunsinger, G.B., Hagopian, W.M., Jahren, A.H., 2010. Offline oxygen isotope analysis of organic compounds with high N: O. *Rapid Commun. Mass Spectrom.* 24 (21), 3182–3186.
- Jackson, P., Cavellier, J., Goldstein, G., Meinzer, F., Holbrook, N., 1995. Partitioning of water resources among plants of a lowland tropical forest. *Oecologia* 101 (2), 197–203.
- Kahmen, A., et al., 2008. Effects of environmental parameters, leaf physiological properties and leaf water relations on leaf water $\delta^{18}\text{O}$ enrichment in different *Eucalyptus* species. *Plant Cell Environ.* 31 (6), 738–751.
- Kanner, L.C., Buenning, N.H., Stott, L.D., Timmermann, A., Noone, D., 2014. The role of soil processes in $\delta^{18}\text{O}$ terrestrial climate proxies. *Global Biogeochemical Cycles* 28 (3), 239–252.
- Leite, E.J., 2005. State-of-knowledge on *Amburana cearensis* (Fr. Allem.) AC Smith (Leguminosae: Papilionoideae) for genetic conservation in Brazil. *J. Nat. Conserv.* 13 (1), 49–65.
- Li, Z., Nakatsuka, T., Sano, M., 2015. Tree-ring cellulose $\delta^{18}\text{O}$ variability in pine and oak and its potential to reconstruct precipitation and relative humidity in central Japan. *Geochem. J.* 49 (2), 125–137.
- Ligges, U., et al., 2015. Package 'Signal': Signal Processing.
- Loader, N., et al., 2014. Simultaneous determination of stable carbon, oxygen, and hydrogen isotopes in cellulose. *Anal. Chem.* 87 (1), 376–380.
- Marshall, J.D., Monsereud, R.A., 2006. Co-occurring species differ in tree-ring $\delta^{18}\text{O}$ trends. *Tree Physiol.* 26 (8), 1055–1066.
- Morales, M.S., Villalba, R., Grau, H.R., Paolini, L., 2004. Rainfall-controlled tree growth in high-elevation subtropical treelines. *Ecology* 85 (11), 3080–3089.
- Offermann, C., et al., 2011. The long way down – are carbon and oxygen isotope signals in the tree ring uncoupled from canopy physiological processes? *Tree Physiol.* 31 (10), 1088–1102.
- Peterson, T.C., Vose, R.S., 1997. An overview of the global historical climatology network temperature database. *Bull. Am. Meteorol. Soc.* 78 (12), 2837–2849.
- Pierrehumbert, R.T., 1999. Huascanan $\delta^{18}\text{O}$ as an indicator of tropical climate during the Last Glacial Maximum. *Geophys. Res. Lett.* 26 (9), 1345–1348.
- Pons, T.L., Helle, G., 2011. Identification of anatomically non-distinct annual rings in tropical trees using stable isotopes. *Trees* 25 (1), 83–93.
- Poussart, P.F., Evans, M.N., Schrag, D.P., 2004. Resolving seasonality in tropical trees: multi-decade, high-resolution oxygen and carbon isotope records from Indonesia and Thailand. *Earth Planet. Sci. Lett.* 218 (3), 301–316.
- Priya, P., Bhat, K., 1998. False ring formation in teak (*Tectona grandis* L.f.) and the influence of environmental factors. *For. Ecol. Manag.* 108 (3), 215–222.
- R Development Core Team, 2015. *R: A Language and Environment for Statistical Computing*. R Foundation for Statistical Computing, Vienna, Austria.
- Reynolds-Henne, C.E., Saurer, M., Siegwolf, R.T., 2009. Temperature versus species-specific influences on the stable oxygen isotope ratio of tree rings. *Trees* 23 (4), 801–811.
- Risi, C., Bony, S., Vimeux, F., 2008. Influence of convective processes on the isotopic composition ($\delta^{18}\text{O}$ and δD) of precipitation and water vapor in the tropics: 2. Physical interpretation of the amount effect. *J. Geophys. Res. Atmos.* 113 (D19).
- Roden, J.S., Lin, G., Ehleringer, J.R., 2000. A mechanistic model for interpretation of hydrogen and oxygen isotope ratios in tree-ring cellulose. *Geochim. Cosmochim. Acta* 64 (1), 21–35.
- Rozanski, K., Araguás-Araguás, L., Gonfiantini, R., 1993. Isotopic patterns in modern global precipitation. *Climate Change in Continental Isotopic Records*, pp. 1–36.
- Salati, E., Dall'Olio, A., Matsui, E., Gat, J.R., 1979. Recycling of water in the Amazon Basin: an isotopic study. *Water Resour. Res.* 15 (5), 1250–1258.
- Saurer, M., et al., 2008. An investigation of the common signal in tree ring stable isotope chronologies at temperate sites. *J. Geophys. Res. Biogeosci.* 113 (G4).
- Schollau, K., et al., 2013. Multiple tree-ring chronologies (ring width, $\delta^{13}\text{C}$ and $\delta^{18}\text{O}$) reveal dry and rainy season signals of rainfall in Indonesia. *Quat. Sci. Rev.* 73, 170–181.
- Schöngart, J., Piedade, M.T.F., Ludwigshausen, S., Horna, V., Worbes, M., 2002. Phenology and stem-growth periodicity of tree species in Amazonian floodplain forests. *J. Trop. Ecol.* 18 (04), 581–597.
- Schwendenmann, L., Pendall, E., Sanchez-Bragado, R., Kunert, N., Hölscher, D., 2014. Tree water uptake in a tropical plantation varying in tree diversity: interspecific differences, seasonal shifts and complementarity. *Ecohydrology* 8 (1), 1–12.
- Singer, M.B., et al., 2013. Contrasting water-uptake and growth responses to drought in co-occurring riparian tree species. *Ecohydrology* 6 (3), 402–412.
- van der Sleen, P., Groenendijk, P., Zuidema, P.A., 2015. Tree-ring $\delta^{18}\text{O}$ in African mahogany (*Entandrophragma utile*) records regional precipitation and can be used for climate reconstructions. *Glob. Planet. Chang.* 127, 58–66.
- Soliz, C., et al., 2009. Spatio-temporal variations in *Polylepis tarapacana* radial growth across the Bolivian Altiplano during the 20th century. *Palaeogeogr. Palaeoclimatol. Palaeoecol.* 281 (3–4), 296–308.
- Song, X., Clark, K.S., Helliker, B.R., 2014a. Interpreting species-specific variation in tree-ring oxygen isotope ratios among three temperate forest trees. *Plant Cell Environ.* 37 (9), 2169–2182.

- Song, X., Farquhar, G.D., Gessler, A., Barbour, M.M., 2014b. Turnover time of the non-structural carbohydrate pool influences $\delta^{18}\text{O}$ of leaf cellulose. *Plant Cell Environ.* 37 (11), 2500–2507.
- Song, X., Barbour, M.M., Farquhar, G.D., Vann, D.R., Helliker, B.R., 2013. Transpiration rate relates to within- and across-species variations in effective path length in a leaf water model of oxygen isotope enrichment. *Plant Cell Environ.* 36 (7), 1338–1351.
- Speer, J.H., 2010. *Fundamentals of Tree-Ring Research*. The University of Arizona Press.
- Stahle, D.W., 1999. Useful strategies for the development of tropical tree-ring chronologies. *IAWA J.* 20 (3), 249–253.
- Sternberg, L., 2009. Oxygen stable isotope ratios of tree-ring cellulose: the next phase of understanding. *New Phytol.* 181 (3), 553–562.
- Sturm, C., Hoffmann, G., Langmann, B., 2007. Simulation of the stable water isotopes in precipitation over South America: comparing regional to global circulation models. *J. Clim.* 20 (15), 3730–3750.
- Tang, K., Feng, X., 2001. The effect of soil hydrology on the oxygen and hydrogen isotopic compositions of plants' source water. *Earth Planet. Sci. Lett.* 185 (3), 355–367.
- Treydte, K., et al., 2014. Seasonal transfer of oxygen isotopes from precipitation and soil to the tree ring: source water versus needle water enrichment. *New Phytol.* 202 (3), 772–783.
- Whitmore, T., 1998. *An Introduction to Tropical Rain Forests*. Clarendon Press.
- Wieloch, T., Helle, G., Heinrich, I., Voigt, M., Schyma, P., 2011. A novel device for batch-wise isolation of α -cellulose from small-amount wholewood samples. *Dendrochronologia* 29 (2), 115–117.
- Wigley, T.M., Briffa, K.R., Jones, P.D., 1984. On the average value of correlated time series, with applications in dendroclimatology and hydrometeorology. *J. Clim. Appl. Meteorol.* 23 (2), 201–213.
- Worbes, M., 1999. Annual growth rings, rainfall-dependent growth and long-term growth patterns of tropical trees from the Caparo Forest Reserve in Venezuela. *J. Ecol.* 87 (3), 391–403.
- Worbes, M., 2002. One hundred years of tree-ring research in the tropics – a brief history and an outlook to future challenges. *Dendrochronologia* 20 (1), 217–231.
- Worbes, M., Junk, W.J., 1989. Dating tropical trees by means of ^{14}C from bomb tests. *Ecology* 70 (2), 503–507.
- Xu, C., Sano, M., Nakatsuka, T., 2011. Tree ring cellulose $\delta^{18}\text{O}$ of *Fokienia hodginsii* in northern Laos: a promising proxy to reconstruct ENSO? *J. Geophys. Res.* 116 (D24).
- Zhang, K., et al., 2015. The Fate of Amazonian Ecosystems over the Coming Century Arising from Changes in Climate, Atmospheric CO₂, and Land use. *Global change biology*.
- Zuidema, P.A., Brienen, R.J., Schöngart, J., 2012. Tropical forest warming: looking backwards for more insights. *Trends Ecol. Evol.* 27 (4), 193–194.